

Study of nanofiber scaffolds of PAA, PAA/CS, and PAA/ALG for its potential use in biotechnological applications

Rodolfo Daniel Velasco-Barraza, Ricardo Vera-Graziano, Eduardo Alberto López-Maldonado, Mercedes Teresita Oropeza-Guzmán, Syed G. Dastager, Adriana Álvarez-Andrade, Ana Leticia Iglesias & Luis Jesús Villarreal-Gómez

To cite this article: Rodolfo Daniel Velasco-Barraza, Ricardo Vera-Graziano, Eduardo Alberto López-Maldonado, Mercedes Teresita Oropeza-Guzmán, Syed G. Dastager, Adriana Álvarez-Andrade, Ana Leticia Iglesias & Luis Jesús Villarreal-Gómez (2018) Study of nanofiber scaffolds of PAA, PAA/CS, and PAA/ALG for its potential use in biotechnological applications, International Journal of Polymeric Materials and Polymeric Biomaterials, 67:13, 800-807, DOI: [10.1080/00914037.2017.1378887](https://doi.org/10.1080/00914037.2017.1378887)

To link to this article: <https://doi.org/10.1080/00914037.2017.1378887>



Accepted author version posted online: 14 Sep 2017.
Published online: 23 Oct 2017.



Submit your article to this journal [↗](#)




Article views: 120



View Crossmark data [↗](#)



Study of nanofiber scaffolds of PAA, PAA/CS, and PAA/ALG for its potential use in biotechnological applications

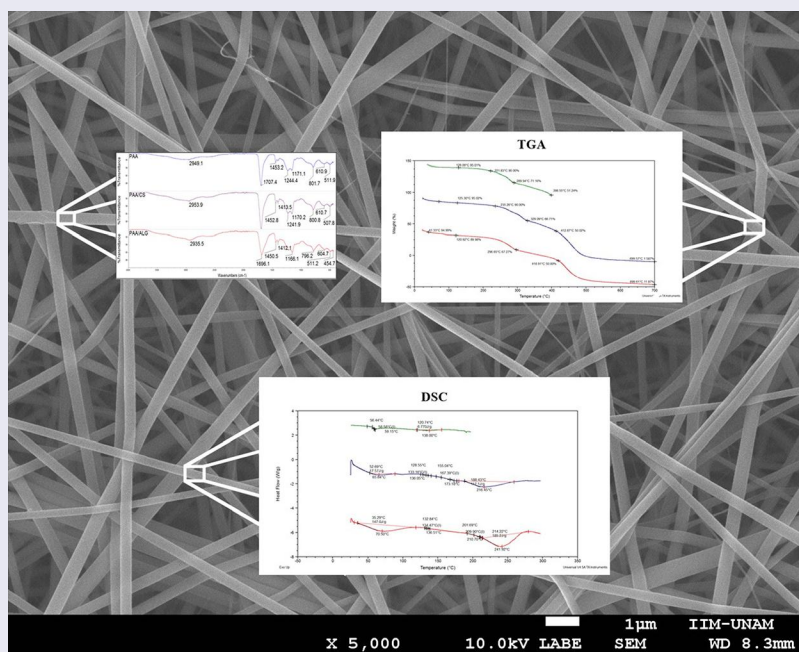
Rodolfo Daniel Velasco-Barraza^a, Ricardo Vera-Graziano^b, Eduardo Alberto López-Maldonado^c, Mercedes Teresita Oropeza-Guzmán^d, Syed G. Dastager^e, Adriana Álvarez-Andrade^a, Ana Leticia Iglesias^a and Luis Jesús Villarreal-Gómez^{a,c} 

^aEscuela de Ciencias de la Ingeniería y Tecnología, Universidad Autónoma de Baja California, Tijuana, Baja California, México; ^bInstituto de Investigaciones en Materiales, Universidad Nacional Autónoma de México, Distrito Federal, México; ^cFacultad de Ciencias Químicas e Ingeniería, Universidad Autónoma de Baja California, Tijuana, Baja California, México; ^dCentro de Graduados, Instituto Tecnológico de Tijuana, Tijuana, Baja California, México; ^eNational Collection of Industrial Microorganisms (NCIM), CSIR-National Chemical Laboratory, Pune, Maharashtra, India

ABSTRACT

In recent times, electrospun nanofibers have been widely studied from several biotechnological approaches; in this work, poly(acrylic acid) (PAA) solutions mixed with chitosan and alginate were electrospun and characterized to determine the behavior of these fibers when used in combination with bacteria, different samples were incubated with the bacterial strains: *Streptomyces* spp., *Micromonospora* spp., and *Escherichia coli* and a OD600 test was performed. The formation of nanofibers via electrospinning and the physicochemical properties of the obtained fibers were evaluated. Results showed that the presence of chitosan enhanced the thermal stability of PAA, since PAA/alginate fibers lost 5% of their mass at 41°C, whereas PAA/chitosan lost this amount at around 125°C. The fibers demonstrated suitable characteristics to be used as a bacteria bioreactor.

GRAPHICAL ABSTRACT



Abbreviations: ALG, alginate; *B. elkani*, *Bradyrhizobium elkani*; *B. japonicum*, *Bradyrhizobium japonicum* β -TCP, β -tricalcium phosphate; CAS, chemical abstracts service; CS, chitosan; DSC, differential scattering calorimetry; *E. coli*, *Escherichia coli*; FTIR, Fourier transform infrared spectroscopy; Tg, glass transition; TGA, thermogravimetric analysis; *S. albus*, *Staphylococcus epidermidis*; SEM, scanning electron microscopy; SHE, synthetic human elastin; PAA, poly(acrylic acid); PEO, poly(ethylene oxide); PLLA/Hap, poly(L-lactic acid)/hydroxyapatite; PPF, poly(propylene fumarate); *P. fluorescens*, *Pseudomonas fluorescens*; *Z. mobilis*, *Zymomonas mobilis*

ARTICLE HISTORY

Received 8 May 2017
Accepted 9 September 2017

KEYWORDS

Alginate; characterization; chitosan; Electrospun fibers; poly(acrylic acid)

1. Introduction

In recent years, electrospinning has evolved into a solid and reliable technique used in diverse applications, allowing the production of nanometric fibers at a moderately industrial scale [1,2]. Although the applications of the nanofibers have been increasing through the years, biomedical research is where great advances have been reported [3]. For example, in tissue engineering, electrospun scaffolds are used to give support to cells while they generate their extracellular matrix (which could have been destroyed by injuries, sicknesses, or genetic defects), without generating an immune response [4–6]. These electrospun scaffolds have also been used for repairing peripheral nerves [7], in osteoblasts cultures [8], as vascular grafts [9], muscle cell regeneration [10], and wound dressings [11].

Nanofibers have also been widely used as drug-delivery systems for localized cancer treatment. The drug, 1,3-bis(2-chloroethyl)-1-nitrosourea used for glioma treatment, is normally administered by intravenous perfusion. Its half-life is close to 20 min after its administration, according to the drug report [12]. However, when used together with electrospun scaffolds, the delivery time can be maintained up to 10 h [13].

The same problem occurs with other anticancer compounds, such as titanocene dichloride ($(\eta^5\text{-C}_5\text{H}_5)_2\text{TiCl}_2$) which is used to treat lung tumors; its delivery and stabilization can be achieved when combined with nanofibers [14]. In addition, nanofibers produced by two or more polymers have been used to diminish the side effects of anticancer drugs, like the ones produced by Brefeldin ($\text{C}_{16}\text{H}_{24}\text{O}_4$) [15].

Nanofibers have been used in environmental applications to understand the behavior of bacteria and their environment. Given the high porosity and wider contact area of the scaffold, an increase in microorganism's interaction with other substances is possible, as well as the increase in the bacterial survivability in adverse environments. Biotechnology usually uses scaffolds to contain or filtrate bacteria from a medium [16].

The first tests to encapsulate biological material were performed with *E. coli*, *Staphylococcus epidermidis*, and viruses (T4, T7, and λ). Although *E. coli* had less viability than *S. albus*, the study helped to demonstrate that bacteria could be encapsulated in electrospun nanofibers, in contrast to viruses, which showed a low survivability [17]. These results conducted to test with probiotic bacteria like *Bifidobacterium animalis lactis* Bb12, a bacterium living in human intestines

that facilitates the correct assimilation of lactose. These bacteria could be preserved for 130 days at 4°C when contained in nanofibers [18].

The contention of bacteria in scaffolds has been tested for its use in bioreactors because it assures the presence of microorganisms in a determined area. *Pseudomonas fluorescens*, *Zymomonas mobilis*, and *E. coli* were immobilized in nanofibers; *Z. mobilis* remained viable in 93% and after days of preservation, it was later used as fermenter and its metabolism was not affected [19]. This capability was tested with other polymers using *E. coli* for Atrazine degradation, thus demonstrating its usefulness as a bioremediation technique [20].

Electrospun bacteria have also been reported in agricultural applications. For example, bacteria such as *Bradyrhizobium japonicum* and *Bradyrhizobium elkani* living in the rhizosphere whose role is nitrogen fixation influence plant growth. Adverse soil conditions affect the presence of bacteria; nonetheless, when contained within water-retaining polymers, the strains increase its survival capacity [21]. In our study, three biopolymers were evaluated: poly(acrylic acid) (PAA), poly(acrylic acid)/chitosan (PAA/CS), and poly(acrylic acid)/alginate (PAA/ALG) for its potential use in biotechnological applications (Figure 1).

In the biomaterials research field, PAA is used to build composite biomaterials with hydroxyapatite. Other applications include the study of the diffusion of hydrogel with poly(vinyl alcohol) (PVA) and the synthesis of poly(N-isopropyl acrylamide), and PAA copolymer blocks, which respond to changes in pH and temperature; the preparation of copolymer blocks of oligo (methyl methacrylate) and PAA has been used for drug-delivery systems of hydrophobic drugs, among others [22,23]. Similarly, chitosan (CS) is biocompatible, antibacterial, and biodegradable, so it can be used for various applications such as water treatment, chromatography, cosmetic additive, antibacterial textiles, photographic paper, biodegradable films, biomedical devices, and implanted microcapsules for the controlled release of medicines [22]. Regarding alginate's applications, it can be used in food, textile, and pharmaceutical industry because of its viscosity and properties as a gelling agent [24].

Marine actinomycetes are considered as valuable sources of new compounds for therapeutic use. *Micromonospora* spp. and *Streptomyces* spp. have started to play an important role in the production of antimicrobial compounds and antibiotics

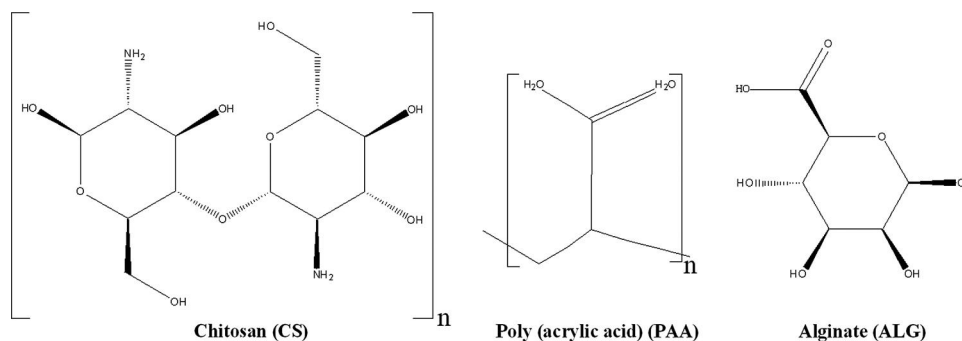


Figure 1. Chemical structures of PAA, CS, and ALG. Note: ALG, alginate; CS, chitosan; PAA, poly(acrylic acid).

[25,26]. However, there are usually problems with the culture of these bacteria due to their specific necessities [27]. Electrospun materials within the cultures open a path to study the interactions of the bacteria with nanofibers and could also introduce a new way to deliver the products needed in the culture of these bacteria.

2. Experimental

Poly(acrylic acid) solution (CAS No. 9003-01-4), $M_w \sim 100,000$, 35% wt., chitosan (CS) (CAS No. 9012-76-4), medium molecular weight, sodium alginate (ALG) (CAS No. 9005-38-3) from Sigma Aldrich and glacial acetic acid (CAS No. 64-19-7) from Jalmek Co. also *Streptomyces* spp. and *Micromonospora* spp. from seawater and *E. coli* from wastewater were used.

2.1. Polymer preparation

Poly(acrylic acid) was used as received. Chitosan was dissolved at 2% (w/v) solution in acetic acid at 90% with constant stirring. ALG was dissolved at 10% (w/v) solution with distilled water under constant stirring. After this, PAA/CS and PAA/ALG were combined in a 3:1 (v/v) proportion by stirring until a homogenous solution was obtained. To eliminate air bubbles, the solutions were centrifuged for a minute.

2.2. Polymer electrospinning

The PAA and PAA/CS electrospinning was performed at 20 kV, with a tip-collector distance of 10 cm and a flow rate of 0.2 mL h^{-1} . For the PAA/ALG electrospinning, only the flow rate was changed from 0.2 mL h^{-1} to 0.3 mL h^{-1} . For all the procedures, humidity was kept under 45%.

2.3. Fourier transform infrared spectroscopy

Spectra of the samples were obtained using a Fourier transform infrared spectroscopy (FTIR) Spectrometer (Spectrum Two, Perkin Elmer), from 4000 cm^{-1} to 400 cm^{-1} . Changes in the spectrum of PAA when combined with the other two polymers were analyzed in the obtained samples using FTIR spectroscopy.

2.4. Scanning electron microscopy

The fibers obtained *via* electrospinning were studied in more detail using a scanning electron microscope (JEOL JSM

7600 F) at different acceleration voltages, ranging from 5 kV to 10 kV. A gold coating was applied to the samples through sputtering, to increase the quality of the obtained image.

2.5. Thermogravimetric analysis and differential scanning calorimetry

TGA was performed with TGA Q5500 (TA Instruments), with a heating rate of $10^\circ\text{C min}^{-1}$, ranging from 25°C to 700°C under nitrogen atmosphere. Differential scanning calorimetry (DSC) was performed with DSC Q5000 (TA Instruments), with a heating rate of $10^\circ\text{C min}^{-1}$ from 25°C to 300°C under nitrogen atmosphere.

2.6. Bacterial culture and fiber evaluation

Micromonospora spp. and *Streptomyces* spp. were cultured in A1 medium at 25°C for 24 h and *E. coli* was cultured in LB medium at 37°C for 24 h. Circular samples of a diameter of 0.5 cm were taken from each combination of polymers and put into a 96-well plate. Over them, $900 \mu\text{L}$ of A1 medium and $100 \mu\text{L}$ of each cultured medium were put over the fibers and the plate was cultured at 37°C for 1 h. After that, OD_{600} was performed.

3. Results

3.1. Morphology by scanning electron microscopy

At first sight, PAA fibers showed a uniform distribution. However, a deeper analysis revealed great variation in the diameter distribution. In contrast to PAA fibers, PAA/CS and PAA/ALG fibers had higher uniformity, with traces of even smaller diameter fibers (Figure 2). PAA/ALG fibers had the smallest diameter out of the three samples.

The measured mean diameter and porosity are shown in Table 1.

3.2. Chemical analysis by Fourier transform infrared spectroscopy

Fourier transform infrared spectroscopy spectra of the PAA, PAA/CS, and PAA/ALG nanofibers are shown in Figure 3. Only slight changes were observed when the spectra are compared. The peaks between 2953 cm^{-1} – 2935 cm^{-1} correspond to the stretching of $-\text{OH}$ groups in PAA, CS, and ALG. The ones present between 1710 cm^{-1} and 1696 cm^{-1} seem to correspond to $-\text{COOH}$ groups stretching; since PAA contains a

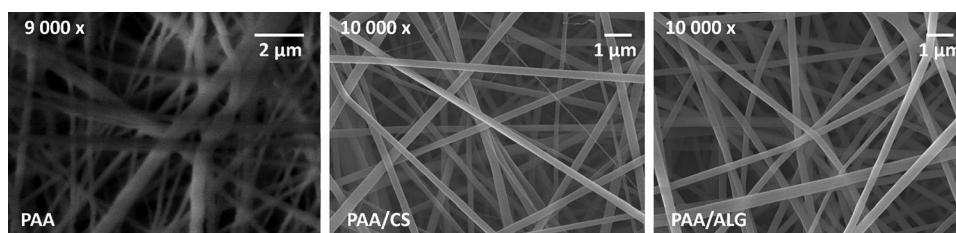


Figure 2. SEM images of PAA, PAA/CS, and PAA/ALG nanofibers. Note: PAA, poly(acrylic acid); PAA/ALG, poly(acrylic acid)/alginate; PAA/CS, poly(acrylic acid)/chitosan; SEM, scanning electron microscopy.

Table 1. Average diameter of nanofibers and porosity percentage of electrospun samples.

Sample	Average fiber diameter	Porosity (%)
PAA	495.03 nm \pm 125.41	45.77
PAA/CS	337.86 nm \pm 61.62	44.76
PAA/ALG	278.52 nm \pm 64.33	42.38

PAA, poly(acrylic acid); PAA/CS, poly(acrylic acid)/chitosan; PAA/ALG, poly(acrylic acid)/alginate.

large amount of carboxylic acid groups that might interact, a high-intensity peak is observed. The PAA/CS sample, however, shows a higher peak compared to the PAA sample, probably showing not only an interaction between carboxylic groups in PAA, but also with certain areas within the CS contained in the sample. In the PAA/ALG, a reduction and broadening of this peak could indicate hydrogen-bonding formation. However, presence of sodium contained in ALG might partially disturb the stretching of carboxylic groups in PAA. The region between 1800 cm^{-1} and 1500 cm^{-1} corresponds to the carboxylic acids and amide groups, but

only an intense peak is observed around 1700 cm^{-1} . In PAA/ALG, the intensity of this peak decreases while its thickness increases compared to the PAA/CS spectrum.

Peaks around 1450 cm^{-1} correspond to C–H bonds bending, which were present in all the samples; those around 1412 cm^{-1} correspond to –OH bending in carboxylic acids. Finally, the peaks between 1171 cm^{-1} and 1166 cm^{-1} can be related to the C–O bond in carboxylic acids of PAA. The similarity between the remaining peaks might only indicate that they all belong to PAA.

3.3. Thermal properties

3.3.1. Thermogravimetric analysis

The three samples followed similar decomposition patterns; however, thermal stability was quite different. The PAA/ALG nanofibers lost 5% of its weight at about 41°C ; while the losses of the PAA and PAA/CS samples occurred close to 125°C . PAA/ALG lost a 10% of weight at 121°C , followed

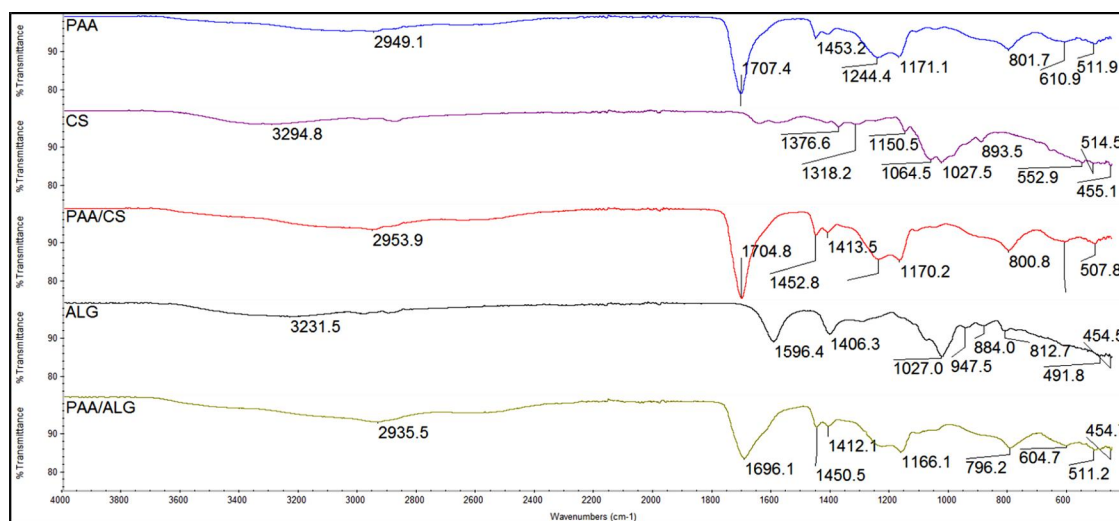


Figure 3. FTIR spectra of PAA, CS, ALG, PAACS, and PAAALG nanofibers. Note: ALG, alginate; FTIR, Fourier transform infrared spectroscopy; PAA, poly(acrylic acid); PAA/ALG, poly(acrylic acid)/alginate; PAA/CS, poly(acrylic acid)/chitosan.

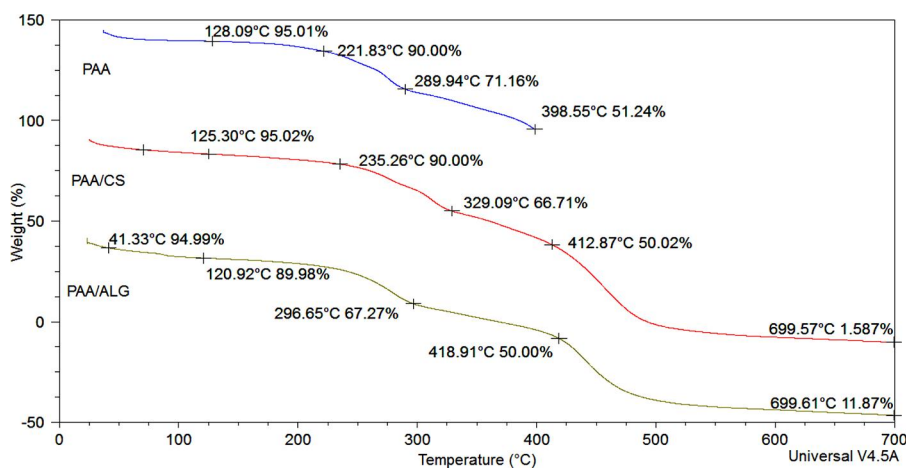


Figure 4. TGA plots of PAA, PAA/CS, and PAA/ALG nanofibers. Note: PAA, poly(acrylic acid); PAA/ALG, poly(acrylic acid)/alginate; PAA/CS, poly(acrylic acid)/chitosan; TGA, Thermogravimetric analysis.

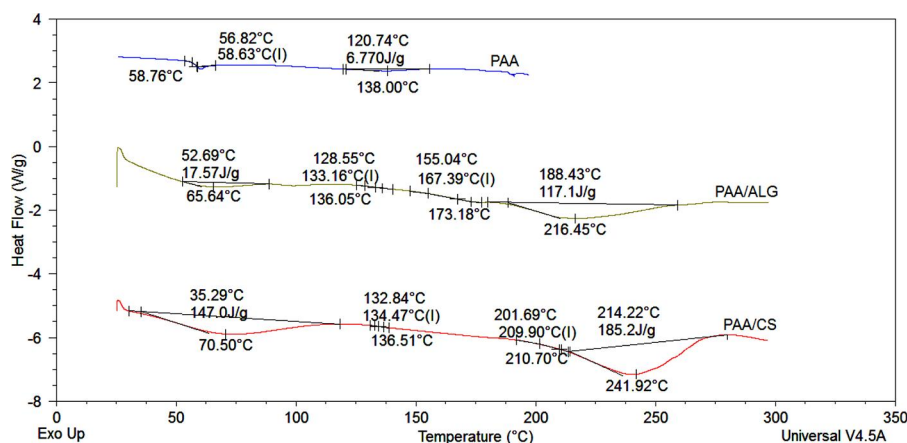


Figure 5. DSC plots of PAA, PAA/CS, and PAA/ALG nanofibers. Note: DSC, differential scanning calorimetry; PAA, poly(acrylic acid); PAA/ALG, poly(acrylic acid)/alginate; PAA/CS, poly(acrylic acid)/chitosan.

by PAA at 222°C and PAA/CS at 235°C. The 50% weight loss threshold was observed at 398°C in PAA, at 418.87°C in PAA/CS and at 418.91°C in PAA/ALG samples. Apparently, PAA/ALG left more residues than PAA/CS, probably due to sodium contained in the ALG (Figure 4).

3.3.2. Differential scanning calorimetry

The PAA nanofibers exhibited a glass transition temperature, T_g , at around 58°C. PAA/ALG nanofibers had two T_g , the first one at 133°C and a second one at 167°C. A desorption stage was also observed at 66°C. PAA/CS also showed two T_g one at 134°C and the other at 210°C, with the desorption stage at 70.5°C (Figure 5).

3.4. Bacterial culture and fiber evaluation

Compared to control measurements, almost all bacterial samples show a reduction in its absorbance value in a considerable

amount. *Micromonospora* spp. decreased its absorbance value to more than a half when exposed to PAA/CS going from 0.092 to 0.038. *Streptomyces* spp. on the other hand exhibits an increase in its absorbance value from 0.026 to 0.033 when exposed to PAA/ALG. Although *Escherichia coli* decreased its absorbance value in all the samples, it is highly pronounced on PAA, where the value goes from 0.056 to 0.006 (Figure 6).

4. Discussion

4.1. Morphological characteristics

PAA electrospinning tends to fail in a high humidity environment due to polymer's hydrophilic nature; hence, a low humidity value allowed the electrospinning procedure. Presence of CS and ALG in the solution increased the PAA's "electrospinnability," thus favoring the fabrication of thinner fibers.

A comparison among this study's fibers average diameter with those in other studies showed that PAA nanofibers of

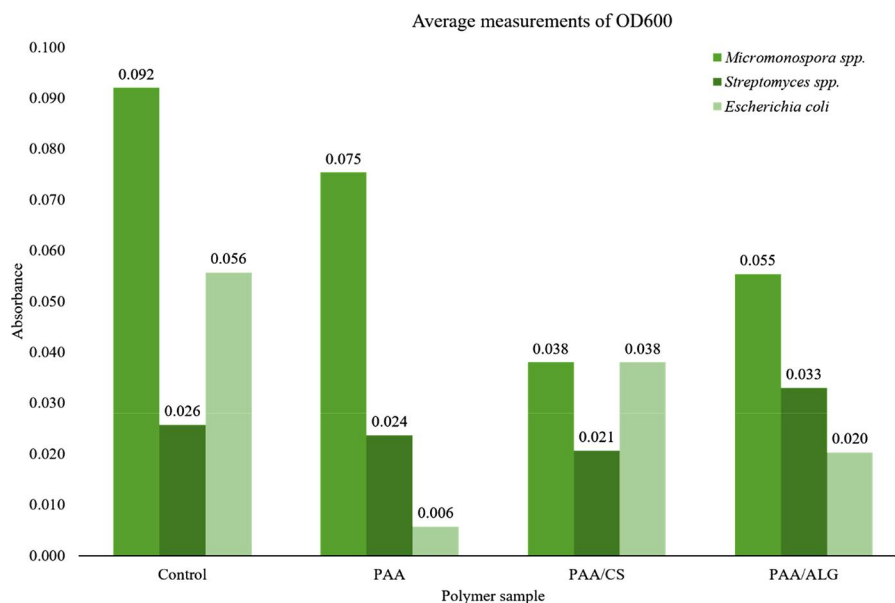


Figure 6. Bacterial growth measurement affected by PAA, PAA/CS and PAA/ALG nanofibers presence in culture plates (600 nm). Note: PAA, poly(acrylic acid); PAA/ALG, poly(acrylic acid)/alginate; PAA/CS, poly(acrylic acid)/chitosan.

495 ± 125 nm accounted for almost half (820 nm) the diameter of ones previously reported [28]. The average diameter reported for PAA/CS nanofibers has been 215 nm, but these nanofibers were prepared through an electrostatic interaction process by adding succinic acid as a branch promoter [29]. The fibers obtained in this study have an average diameter of 339 ± 61 nm.

In the PAA/ALG nanofibers case, a comparison with previous studies could not be made since combination of these two substances has not been reported in scientific literature until now. ALG has been electrospun with glycerol, PVA, and poly(ethylene oxide) [30], but not with PAA.

Improvements in nanofibers characteristics when ALG is included in the formulations have already been reported. These improvements include biocompatibility and mechanical properties [31,32], great potential as a cell scaffold for the regeneration of several tissues, crosslinking of nanofibers and enhancement of cell adhesion [33,34].

Scanning electron microscopy analysis indicated that PAA/CS and PAA/ALG fibers had smaller diameter than PAA nanofibers. This effect can be associated with the increase in ions in the solutions improving conductivity and solvent evaporation.

Regarding porosity, scaffolds with large pore size tend to successfully deliver biomolecules such as proteins, genes, and cells. Additionally, connected pores guarantee good nutrients exchange. Despite this, it is necessary to equilibrate porosity with mechanical properties, as porosity increases in the scaffolds, mechanical properties tend to decrease, and vice-versa [34].

Our nanofiber scaffolds showed a 44.3% average porosity among the three samples. This porosity can be suitable for bone formation and infiltration of dermal fibroblasts (Table 2).

It is convenient to consider the chemical combination of the biomaterials used, as well as their biocompatibility. Villarreal-Gómez et al. [39–41] evaluated the biocompatibility of poly(L-lactic acid)/hydroxyapatite for bone tissue engineering, arguing that the chemical composition of the scaffolds is very important for the final tissue engineering application.

It is known that PAA is biocompatible and has been used as coating [42] and as a drug-delivery system [43]. It has also been studied as a super porous hydrogel for microparticles with a good super-disintegrating rate for fast-disintegrating tablets [44], among other applications.

Both chitosan and ALG are biocompatible; chitosan possess antimicrobial activity [45] and ALG can be used as hydrogel and can be applied in wound healing, drug delivery, and tissue engineering. Since ALG keeps a structural similarity to the extracellular matrices in tissues, it can be manipulated to play several important functions [46].

4.2. Chemical structure

The infrared spectrum of the PAA (Figure 3) exhibited similar characteristics to those reported by other authors [47,48].

Poly(acrylic acid)/chitosan spectra show no coincidences with those previously reported [49]. The amide group peaks used to identify CS and were not observed in the spectra. Since the ratio PAA/CS is 3:1, it is possible that the PAA spectra overlap the CS spectra. The most important peaks for identification of CS are the amide group (at 1665 cm⁻¹, 1620 cm⁻¹, and approximately 1325 cm⁻¹), but such peaks could not be visualized in the spectra due to the possible overlapping with the carboxylic groups.

On the other hand, the ALG spectra displayed coincidences with the one reported by Zhang et al [50]. However, the PAA/ALG spectra could be in the same situation of the PAA/CS spectra, because its peaks are not found in literature [51] since the small characteristic peak of the ALG at 840 cm⁻¹ indicates the oxygen bond to sodium and was visualized in the ALG spectrum but not in the PAA/ALG one. Another characteristic to be highlighted is that, in that spectrum, the peak of 1700 cm⁻¹ reduces its intensity and becomes wider than the PAA spectrum.

4.3. Thermal stability

The thermogravimetric analysis of PAA showed behavior differences compared to those reported in Khalid et al. [52]. Data obtained from our analysis indicated a decomposition by stages which is not observed in the referenced work. On the other hand, there was a noticeable faster thermal wear rate due to a considerable amount of mass loss at lower temperature (around 41°C).

Glass transition analysis of PAA/CS nanofibers showed differences compared to the PAA sample; the loss of mass at 10 and 50% occurs at higher temperatures.

Finally, there were differences in the TG analysis of the PAA/ALG sample, comparatively with the PAA and PAA/CS samples. A fast mass loss was observed between 5% and 10%, a slower mass drop occurred close to the 300°C compared to the other two samples, this sample left a larger amount of mass at 700°C compared to the PAA/CS sample. This behavior is different to the one reported by Jeung and Mishra [53].

4.4. Thermal transitions

An endothermic peak was observed at 59°C and a Tg close to 58°C. These transitions are consistent with those reported by

Table 2. Importance of % porosity in biomedical applications.

Biomaterials	Porosity (%)	Application	Reference
Silk fibroin scaffolds	86	Better cell proliferation	[32]
Synthetic human elastin (SHE) scaffolds	34.4	Infiltration of dermal fibroblasts	[33]
PLLA and PLGA scaffolds	87	Formation of cartilage-like tissue	[34]
Poly(propylene fumarate)/β-tricalcium phosphate (PPF/β-TCP) scaffolds	49	Bone formation	[35,37]
Calcium aluminate cylindrical scaffolds	46	Bone formation	[36,38]

PLLA, Poly(L-lactic acid).

PLGA, Poly(lactic-co-glycolic acid).

Khalid et al. [52], who found an endothermic peak at 58°C and a T_g close to 55°C on PAA nanofibers.

Our DSC study showed similar characteristics to those reported by Bekin et al. [54]. Although the first endothermic peak appeared at approximately 30°C below the one reported the second peak appeared at 241.92°C, a temperature close to the one reported (245°C) on PAA/CS nanofibers.

The DSC also showed similar characteristics to the ones reported by Bekin et al. [55], the endothermic peaks at 65.64°C and 216.45°C occurred at the same temperature range (60°C–80°C and 207°C–219°C) on PAA/ALG nanofibers.

4.5. Polymer behavior

Micromonospora spp. cell density is reduced with all the polymer combinations, especially by PAA/CS going from 0.092 to 0.038 after 1 h of incubation. Since already altered by PAA, it is possible that the amount of CS present in the combination increases this effect over the strain, indicating that CS reinforces the bacteriostatic effects as it has been reported [56]. In the case of *Streptomyces* spp., it is relatively unaffected by PAA and PAA/CS, being this one where the higher decrease in cell concentration is seen going from 0.026 to 0.021; it must be noted that interactions with PAA/ALG increase this value from 0.026 to 0.033; therefore, the possibility that *Streptomyces* spp. uses ALG as carbon source arises. Finally, *E. coli* observations seem consistent with other experiments proposed by Santiago-Morales et al. [57], where PAA and PAA/PVA combinations were tested; the presence of other polymers in conjunction with PAA seems to reduce the antibacterial activity of PAA over different bacterial strains.

5. Conclusion

Although the presence of CS and ALG enhanced the thermal stability of PAA nanofibers, this did not occur at low temperatures. PAA/ALG fibers lost a large amount of mass compared to the other fibers at near room temperature. Also, the addition of CS and ALG reduced the nanofibers average diameter with an average porosity of 44.3%. This porosity value seems to be adequate for bone tissue engineering, favoring the idea that its use in biomedical applications might be explored. Formulations of ALG and PAA have not been reported previously, but our analysis of this combination supports the idea that these scaffolds could also be used for tissue engineering as well as drug-delivery systems. Inclusion of these polymers in the nanofibers also favors the formation of thinner fibers. The interaction of the fibers with bacteria do not affect the bacterial cultures in a positive way although there is a possibility where they can be used as tools for keeping cultures free from unwanted strains, as it could be seen with PAA, where it reduced the presence of *E. coli*. Further studies are needed to determine whether these fibers could be useful for these applications.

Funding

Authors thank for financial support to “Consejo Nacional de Ciencia y Tecnología (CONACYT)” for its grant known as “Fondo de Cooperación

Internacional en Ciencia y Tecnología del Conacyt (FONCICYT)” in its grant named as “Convocatoria Conjunta de Movilidad 2015 CONACYT-DST México-India” with CONACYT project number 266380 and SICASPI-UABC number 351/375/E. Also to PAPIIT-UNAM grant IN108116. Moreover, authors thank to Universidad Nacional Autónoma de México and its technicians: QFB Karla Eriseth Reyes Morales (TGA and DSC analysis) and Quim. Miguel Ángel Canseco Martínez (FTIR analysis) and the Centro de Investigación y Desarrollo Tecnológico en Electroquímica S.C.-Tijuana and its technician: Dr. Ricardo Valdez Castro (SEM analysis).

ORCID

Luis Jesús Villarreal-Gómez  <http://orcid.org/0000-0002-4666-1408>

References

- [1] Velasco-Barraza, R. D.; Álvarez Suarez, A. S.; Villarreal Gómez, L. J.; Paz González, J. A.; Iglesias, A. L.; Vera Graziano, R. *Rev. Mex. Ing. Biomed.* **2016**, *37*, 7–16.
- [2] Villarreal-Gómez, L. J.; Cornejo-Bravo, J. M.; Vera-Graziano, R.; Grande, D. *J. Biomater. Sci. Polym. Ed.* **2016**, *27*, 157–176.
- [3] Agarwal, S.; Wendorff, J. H.; Greiner, A. *Polymer (Guildf)*. **2008**, *49*, 5603–5621.
- [4] Liang, D.; Hsiao, B. S.; Chu, B. *Adv. Drug Deliv. Rev.* **2007**, *59*, 1392–1412.
- [5] Sarvari, R.; Sattari, S.; Massoumi, B.; Agbolaghi, S.; Beygi-Khosrowshahi, Y.; Kahaie-Khosrowshahi, A. *J. Biomater. Sci. Polym. Ed.* **2017**, *28*, 1740–1761.
- [6] Sarvari, R.; Akbari-Alanjaraghi, M.; Massoumi, B.; Beygi-Khosrowshahi, Y.; Agbolaghi, S. *New J. Chem.* **2017**, *14*, 6371–6384.
- [7] Bini, T. B.; Gao, S.; Tan, T. C.; Wang, S.; Lim, A.; Hai, L. Ben; Ramakrishna, S. *Nanotechnology* **2004**, *15*, 1459–1464.
- [8] Fujihara, K.; Kotaki, M.; Ramakrishna, S. *Biomaterials* **2005**, *26*, 4139–4147.
- [9] Tillman, B. W.; Yazdani, S. K.; Lee, S. J.; Geary, R. L.; Atala, A.; Yoo, J. *J. Biomaterials* **2009**, *30*, 583–588.
- [10] Aviss, K. J.; Gough, J. E.; Downes, S. *Eur. Cells Mater.* **2010**, *19*, 193–204.
- [11] Abrigo, M.; McArthur, S. L.; Kingshott, P. *Macromol. Biosci.* **2014**, *14*, 772–792.
- [12] Sartorelli, A. C.; Johns, D. G. *Antineoplastic and Immunosuppressive Agents*, 2nd ed.; Springer: Berlin, Heidelberg, 2013.
- [13] Xu, X.; Chen, X.; Xu, X.; Lu, T.; Wang, X.; Yang, L.; Jing, X. *J. Control. Release* **2006**, *114*, 307–316.
- [14] Chen, P.; Wu, Q.-S.; Ding, Y.-P.; Chu, M.; Huang, Z.-M.; Hu, W. *Eur. J. Pharm. Biopharm.* **2010**, *76*, 413–420.
- [15] Liu, W.; Wei, J.; Huo, P.; Lu, Y.; Chen, Y.; Wei, Y. *Mater. Sci. Eng. C* **2013**, *33*, 2513–2518.
- [16] Doyle, J. J.; Choudhari, S.; Ramakrishna, S.; Babu, R. P. *Conf. Papers Mater. Sci.* **2013**, *2013*, 1–14.
- [17] Salalha, W.; Kuhn, J.; Dror, Y.; Zussman, E. *Nanotechnology* **2006**, *17*, 4675–4681.
- [18] López-Rubio, A.; Sanchez, E.; Wilkanowicz, S.; Sanz, Y.; Lagaron, J. M. *Food Hydrocoll.* **2012**, *28*, 159–167.
- [19] Liu, Y.; Ji, Y.; Ghosh, K.; Clark, R. A. F.; Huang, L.; Rafailovich, M. H. *J. Biomed. Mater. Res. - Part A* **2009**, *90*, 1092–1106.
- [20] Tong, H.-W.; Mutlu, B. R.; Wackett, L. P.; Aksan, A. *Mater. Lett.* **2013**, *111*, 234–237.
- [21] Damasceno, R.; Roggia, I.; Pereira, C.; de Sá, E. *Can. J. Microbiol.* **2013**, *59*, 716–719.
- [22] McKenzie, M.; Betts, D.; Suh, A.; Bui, K.; Kim, D. L.; Cho, H. *Molecules* **2015**, *20*, 20397–20408.
- [23] Jiang, X.; Zhai, S.; Jiang, X.; Lu, G.; Huang, X. *Polymer* **2014**, *55*, 3703–3712.
- [24] Hay, I. D.; Rehman, Z. U.; Moradali, M. F.; Wang, Y.; Rehm, B. H. A. *Microb. Biotech.* **2013**, *6*, 637–650.
- [25] Subramani, R.; Aalbersberg, W. *Microb. Res.* **2012**, *167*, 571–580.

- [26] Manivasagan, P.; Venkatesan, J.; Sivakumar, K.; Se-Kwon, K. *Microb. Res.* **2013**, *168*, 311–332.
- [27] Sharma, M.; Dangi, P.; Choudhary, M. *Int. J. Curr. Microbiol. App. Sci.* **2014**, *3*, 801–832.
- [28] Meng, L.; Klinkajon, W.; K-Hasuwan, P.-r.; Harkin, S.; Supaphol, P.; Wnek, G. E. *Polym. Int.* **2015**, *64*, 42–48.
- [29] Wang, J.-W.; Chen, C.-Y.; Kuo, Y.-M. *Polym. Adv. Technol.* **2008**, *19*, 1343–1352.
- [30] Bonino, C. A.; Krebs, M. D.; Saquing, C. D.; Jeong, S. I.; Shearer, K. L.; Alsberg, E.; Khan, S. A. *Carbohydr. Polym.* **2011**, *85*, 111–119.
- [31] Jeong, S. I.; Krebs, M. D.; Bonino, C. A.; Khan, S. A.; Alsberg, E. *Macromol. Biosci.* **2010**, *10*, 934–943.
- [32] Hu, C.; Gong, R. H.; Zhou, F. L. *Int. J. Polym. Sci.* **2015**, *2015*, 1–12.
- [33] Jeong, S. I.; Krebs, M. D.; Bonino, C. A.; Samorezov, J. E.; Khan, S. A.; Alsberg, E. *Tissue Eng. Part A* **2010**, *17*, 59–70.
- [34] Loh, Q. L.; Choong, C. *Tissue Eng. Part B Rev.* **2013**, *19*, 485–502.
- [35] Mandal, B.; Kundu, S. *Biomaterials* **2009**, *30*, 2956.
- [36] Rnjak-Kovacina, J.; Wise, S.; Li, Z.; Maitz, P.; Young, C.; Wang, Y.; Weiss, A. *Biomaterials* **2011**, *32*, 6729.
- [37] Mikos, A.; Temenoff, J. *Electron. J. Biotech.* **2000**, *3*(2), 315–318.
- [38] Moffitt, E. N.; Lin, C. Y.; Krebsbach, P. H.; Hollister, S. J. *52nd Ann. Meet. Ortho. Res. Soc.* **2006**, *52*, 0831.
- [39] Karageorgiou, V.; Kaplan, D. *Biomaterials* **2005**, *26*, 5474–5491.
- [40] Villarreal-Gómez, L. J.; Vera-Graziano, R.; Vega-Ríos, M. R.; Pineda-Camacho, J.; Almanza-Reyes, H.; Mier-Maldonado, P. A.; Cornejo-Bravo, J. M. *J. Mex. Chem. Soc.* **2014**, *58*(4), 435–443.
- [41] Villarreal-Gómez, L. J.; Vera-Graziano, R.; Vega-Ríos, M. R.; Pineda-Camacho, J.; Almanza-Reyes, H.; Mier-Maldonado, P. A.; Cornejo-Bravo, J. M. *Adv. Mater. Res.* **2014**, *976*, 191–195.
- [42] De Giglio, E.; Cafagna, D.; Ricci, M. A.; Sabbatini, L.; Cometa, S.; Ferretti, C.; Mattioli-Belmonte, M. *J. Bioact. Compat. Polym.* **2010**, *25*, 374–391.
- [43] Gebelein, C. G.; Carraher, C. E. *Bioactive Polymeric Systems: An Overview*, 1st ed.; Springer: Boston, Massachusetts, United States, 2012.
- [44] Yang, S.; Fu, Y.; Jeong, S. H.; Park, K. *J. Pharm. Pharma.* **2004**, *56*, 429–436.
- [45] Benhabiles, M. S.; Salah, R.; Lounici, H.; Drouiche, N.; Goosen, M. F. A.; Mameri, N. *Food Hydrocoll.* **2012**, *29*, 48–56.
- [46] Lee, K. Y.; Mooney, D. J. *Prog. Polym. Sci.* **2012**, *37*, 106–126.
- [47] Ghorbaniazar, P.; Sepehrianazar, A.; Eskandani, M.; Nabi-Meibodi, M.; Kouhsoltani, M.; Hamishehkar, H. *Adv. Pharm. Bull.* **2015**, *5*, 269–275.
- [48] Neira, A.; Tarraga, M.; Catalan, R. *J. Chil. Chem. Soc.* **2007**, *52*, 1314–1317.
- [49] Guo, L.; Liu, G.; Hong, R. Y.; Li, H. Z. *Mar. Drugs* **2010**, *8*, 2212–2222.
- [50] Mohamed, S. F.; Mahmoud, G. A.; Taleb, M. F. A. *Monatsh. Chem.* **2013**, *144*, 129–137.
- [51] Zhang, J.; Xu, S.; Zhang, S.; Du, Z. *Iran Polym J* **2008**, *17*, 899–906.
- [52] Moharram, M. A.; Allam, M. A. *J. Appl. Polym. Sci.* **2007**, *105*, 3220–3227.
- [53] Khalid, I.; Ahmad, M.; Usman Minhas, M.; Barkat, K.; Sohail, M. *Adv. Polym. Technol.* **2016**, *0*, 1–11.
- [54] Jeung, S.; Mishra, M. K. *Int. J. Polym. Mater.* **2010**, *60*, 102–113.
- [55] Bekin, S.; Sarmad, S.; Gürkan, K.; Keçeli, G.; Gürdağ, G. *Sensors Actuators B Chem.* **2014**, *202*, 878–892.
- [56] Goy, R. C.; Britto, D.; Assis, O. *Polímeros.* **2009**, *19*, 241–247.
- [57] Santiago-Morales, J.; Amariei, G.; Letón, P.; Rosal, R. *Coll. Surf. B Biointer.* **2016**, *146*, 144–151.